Energy 242 (2022) 122987

Contents lists available at ScienceDirect

Energy

journal homepage: www.elsevier.com/locate/energy

Effect of slickwater-alternate-slurry injection on proppant transport at field scales: A hybrid approach combining experiments and deep learning

Lei Hou [a, *], Yiyan Cheng [b], Xiaoyu Wang [c], Jianhua Ren [b], Xueyu Geng [a, **]

[a] School of Engineering, The University of Warwick, Coventry, CV4 7AL, UK
[b] Research Institute of Exploration & Development, East China Company of SINOPEC, Nanjing, 210011, China
[c] Department of Earth, Environmental and Planetary Sciences, Rice University, Houston, TX, USA

ARTICLE INFO

Article history:
Received 8 June 2021
Received in revised form
7 December 2021
Accepted 20 December 2021
Available online 22 December 2021

Keywords:
Proppant transport
Alternate injection
Proppant ridge
Deep learning
Field scale

ABSTRACT

Proppant transport in underground fractures plays a key role in mitigating sand screen-out and enhancing the stimulated production for hydraulic fracturing. The effects of field pumping schedules, however, are not fully studied. We investigate the effect of slickwater-alternate-slurry injection on proppant transport at field-practical scales. A new hybrid approach is proposed to directly connect experimental studies with field operations, which consists of observation experiments, calculations, and deep learning (DL) workflow. The experiments reveal that the alternate injection induces the unexpected proppant ridge. The modified calculations (considering the ridge height) are proposed to extract features for training the DL algorithm. The workflow predicts the downhole pressure (mainly governed by proppant injection) for error analyses. Approximately 20.2% of the error is eliminated by considering the proppant ridge, thus demonstrating its effect on proppant injection. The predictions are significantly improved in early and late periods of fracturing operations when the fracture is initially created and highly filled. The sensitivity analysis suggests that the pump rate may dominate the ridge height compared with other hydraulic parameters. The study of proppant ridge complements the mechanisms of proppant transport, which is essential for controlling fracturing pressure and boosting the proppant injection.

1. Introduction

The hydraulic fracturing enabled the emergence of the unconventional revolution for shale reservoirs, where the proppant injection is one of the dominant operations [1–3]. It is still challenging to inject proppant under safe operating pressures, particularly with the application of the low-viscosity slickwater [4,5], which makes the studies on proppant transport critical in hydraulic fracturing engineering. Experimental and numerical simulations at different scales, ranging from centimetre-level to meter-level, have revealed the fundamental mechanisms and calculations of proppant accumulating, stratified-flowing, and dune evolution in low-viscosity fracturing fluid (e.g. slickwater) [6,7]. The performance of proppant injection in slickwater is significantly improved by increasing the pumping rate substantially and employing a slickwater-alternate-slurry injection schedule, where phases of slurry and pure slickwater are injected alternately [8,9].

As the massive hydraulic fracturing treatments are increasingly prevalent for unconventional reservoirs, new issues come along, such as the more frequent occurrence of sand screen-out, high operation pressure and insufficient volume of injected proppant [10,11]. Recent efforts demonstrate the effects of fracture morphology, tortuosity, and real rock roughness on the proppant transport [12,13], trying to improve the simulation by considering the fracture features cracked in unconventional formations. Currently, it is still difficult to characterize underground fractures precisely due to the lack of direct measurements [14]. Previous experimental or numerical simulations mainly focus on the fracture parameters (creation, propagation, etc.) [15], material properties (fluid and proppant) and hydraulic parameters (pump rate, sand ratio, etc.) [16]. Most of the studies explore the equilibrium status of

* Corresponding author.
** Corresponding author.
E-mail addresses: lei.hou@warwick.ac.uk (L. Hou), xueyu.geng@warwick.ac.uk (X. Geng).

https://doi.org/10.1016/j.energy.2021.122987
0360-5442/

proppant dune based on a simplified continuous pumping schedule [17,18]. However, the effect of the realistic pumping schedule and the intermediate state of the proppant dune during the alternate injection are not fully investigated, which may be crucial for the proppant transport [19].

We, therefore, propose a new hybrid approach, including experiments, calculations and a deep learning workflow, to study the effect of the alternate pumping schedule on proppant injection at field-practical scales. The observation experiments, simulating the alternate injecting schedules, reveal the new mechanism of proppant dune evolution. The corresponding calculations, quantifying the experimental observations, are proposed and used to extract features for training the algorithm, thus linking the experimental discovery to the deep learning workflow. The Gated Recurrent Units (GRU) algorithm is employed to process the field measurements directly, which bypasses the characterization of fracture networks compared with traditional simulations [10,12]. By converting the pressure (from wellhead to downhole) and controlling the geological uncertainties, the proppant transport in fractures is mainly reflected by the pressure variations in this study. The deep learning workflow, based on traditional and modified calculations, predicts the downhole pressure for error analyses to reveal the effect of the new experimental mechanism. Our hybrid design aims to provide an advanced and practical approach that directly connects laboratory discoveries with field applications. Based on the new approach, the effect of the slickwater-alternate-slurry injection on proppant transport is investigated, which may be significant for the safety of fracturing operation and enhancement of stimulated production.

2. Methodology

There are three main components in our hybrid approach: 1) A single fracture simulator is utilized for experiments of proppant flow, aiming to disclose the evolution of proppant dune that may be induced by the alternate pumping schedule; 2) The modified calculations are proposed to quantify the experimental observations; 3) A deep learning workflow is built by integrating the modified calculations and the GRU algorithm to process the field records and predict the downhole pressure. The prediction errors based on traditional and modified calculations are analyzed to evaluate the effect of the slickwater-alternate-slurry injection on the proppant transport, which is measured by the root mean square error – RMSE [19].

2.1. The concept of the hybrid research approach

A new hybrid approach is employed in this study, consisting of experiments, calculations and a deep learning workflow, as shown in Fig. 1. It validates and analyzes the experimental mechanism based on field records. The experimental simulations are initially carried out to disclose the effect of alternate injection on the evolution of proppant dune. The modified calculations are proposed to quantify the transition state of the proppant dune, then are applied for data preprocessing in the deep learning workflow. The GRU-based workflow predicts the downhole pressure after perforation (defined as DPP) based on field measurements and calculations. Subsequently, the predicting errors based on traditional and modified calculations are compared to demonstrate the effect of the experimental discovery on proppant injection. In the hybrid approach, the modified calculations, motivated by experiments, act as the link between experiments and the deep learning workflow. The GRU workflow directly connects the laboratory study to field cases, providing a more effective framework for testing indoor outcomes at engineering scales.

2.2. Apparatus and materials

The laboratory experiment, using a self-designed apparatus [20], is conducted to simulate the field pumping conditions and test the effect of the alternate injection on the proppant transport (Fig. 2). The slurry and pure slickwater are injected alternately into a $5 \times 50 \times 1000$ mm fracture with a constant pump rate driven by a screw pump. A group of observation windows (45 mm in diameter) is set in pairs on both sides of the fracture simulator to present a clear view of the particle flow and accumulation. Each window is monitored by a camera to record the evolution of the proppant dune in the fracture. The complete appearance of the proppant dune is then facsimiled based on image analyses.

The 40/70 ceramic proppant (3120 kg/m^3 in density) and slickwater (3 mPa s in viscosity) are mixed with proppant at a concentration of 5%. The slurry and pure slickwater are injected alternately into the fracture simulator with a constant pump rate of 0.8 L/min. We manually mix the proppant into the constantly injected slickwater through the blender every 1-min interval to mimic the slickwater-alternate-slurry pumping schedule. The cameras record the evolution of the proppant dune through each window during the injection. The morphology of the entire proppant dune is restored by splicing the pictures from all observation windows. This observational experiment aims to demonstrate the correlation between the dune evolution (geometry) and alternate injecting mode.

2.3. Data collection and denoising

Around 270,000 groups of fracturing measurements are collected from 33 fracturing stages operated in 6 neighbouring wells (A_1 and A_2, B_1 and B_2, C_1 and C_2) that are drilled through the Longmaxi formation, Sichuan basin (Table 1). The original field records include the geological (vertical and well depths), clustering (perforation number) and fracturing measurements (fluid and proppant types, pump rate, proppant concentration and wellhead pressure). The wells are evenly distributed at three platforms (A, B and C). There are 30 stages of fracturing data (from A_1, B_1 and C_1, defined as the training wells, Table 1) selected for training the GRU algorithm. Concurrently, the remaining three stages are defined as the testing stage (Table 1), randomly selected from the neighbour wells (wells A_2, B_2 and C_2).

The fracturing pressure variation is indicative of the proppant transport status [21]. However, the pressure can also be controlled by various factors, including the geological characteristics, variations of the hydrostatic pressure and friction, randomly cracked fracture and its propagation, and human interventions [22,23]. We, therefore, denoise the raw data by 1) proposing predictions (Testing Datasets) based on the neighbour well experiences (Training Datasets), which is beneficial to control the geological uncertainty (Table 1); 2) converting wellhead pressure into the downhole pressure after perforation (DPP) to eliminate the influences of variations in hydrostatic pressure and friction (details of the conversion can be found in the Appendix); 3) trimming the pressure fluctuations occurred at the beginning (creating fracture) and in the end (pump off) of the fracturing operation; 4) repeating the prediction for three times of iterations based on different platforms to average the errors; 5) assuming that the influence of fracture growth during the proppant injection is insignificant. After the data denoising, the DPP is used to evaluate the subsurface proppant transport.

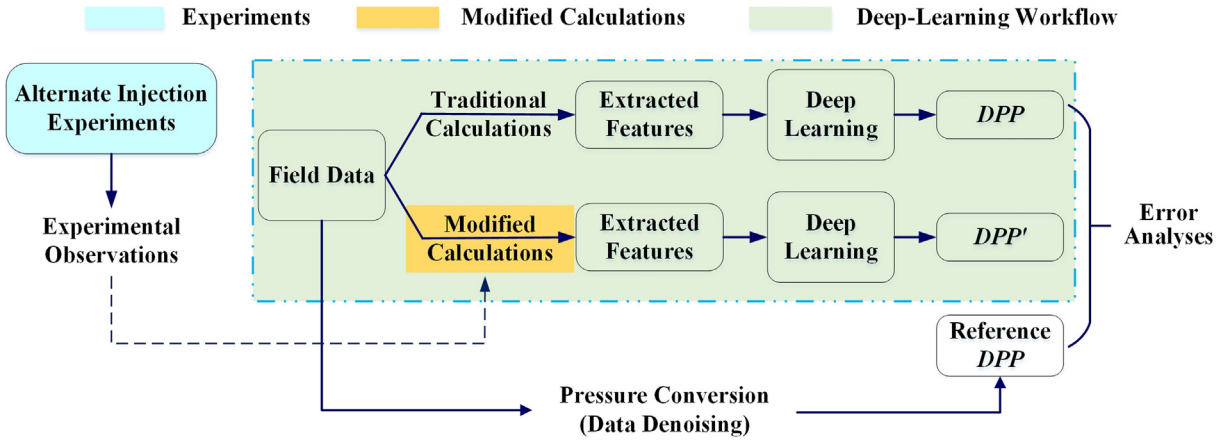

Fig. 1. The hybrid approach, consisting of experiments, calculations and a deep learning workflow. The experiments reveal the transition state of the proppant dune, which is quantified by the modified calculations. The calculations connect the experimental observation and the deep learning workflow. The workflow demonstrates and analyzes the effect of the experimental mechanism at field practical scales.

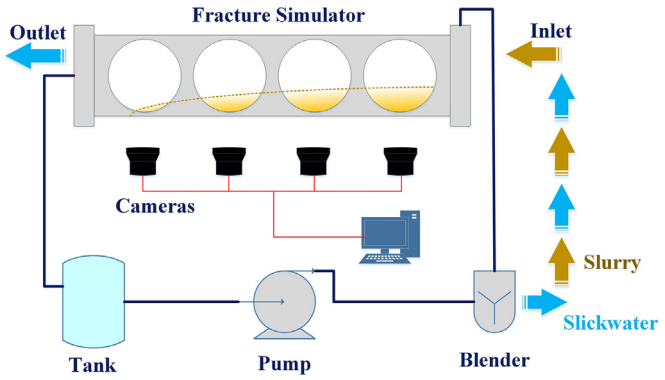

Fig. 2. Schematic of the proppant transport simulator [20] and slickwater-alternate-slurry injections.

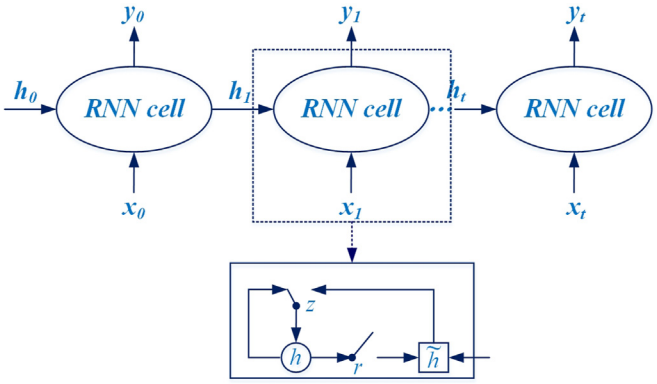

Fig. 3. Architecture of the GRU model. Each cell consists of a three-layer fully connected neural network. x_t represents input features at each time step t, y_t represents prediction at each time step t, h_t, h, $\sim$ h are hidden states. r is the reset gate, where the hidden state is forced to ignore the previous hidden state and reset with the current input. z is the update gate that controls how much information passes from the previous hidden state to the current hidden state [24].

Table 1
Division of training and testing datasets.

	Platform A		Platform B		Platform C	
Wells No.	A_1	A_2	B_1	B_2	C_1	C_2
Training Dataset/Stages	10	/	10	/	10	/
Testing Dataset/Stages	/	1	/	1	/	1

2.4. GRU model

Based on the size of our dataset and the time-dependent nature of the fracking operations, we construct a GRU model building on the previous effort [24]. The GRU algorithm, designed for extracting information from time sequence, has showcased impressive performances in the petroleum engineering area [25,26]. The architecture of the model is shown in Fig. 3. Each GRU model consists of multiple recurrent neural network (RNN) cells in a time-step manner. The input, including fracturing measurements (x_t) at a certain time step t, can affect the hidden state (h_t) of the RNN cell at the time step of t. The updated hidden state (h_t) combined with the following fracture measurements (x_{t+1}) are then fed to the next RNN cell that will predict the successive pressure result (y_{t+1}). In essence, one GRU model represents one operation stage, where the in-situ measurements at each time step (x_t, $t = 0$s, 1s, 2s, …) are fed to each RNN cell of the model, yielding a downhole pressure after perforation (DPP) for each corresponding time step (y_t, $t = 0$s, 1s, 2s, …). The trained weights of neural units of each model are saved for each fracturing stage. All input variables are standardized by removing the mean and scaling to unit variance.

According to the previous pre-trained models [19], a three-layer (including the output layer) GRU is established with the activation function 'ReLu' operating in each layer. The dropouts (the rate of 0.2) are set after the first and hidden layers to avoid overfitting [27]. The 'Adam' optimizer is selected to compile the model [28]. A callback function is applied to return and automatically update the learning rate [29]. The batch size (50) and epochs (30) are optimized by the Grid search and Walk-forward validation [30–32].

3. Results

The evolution of the proppant dune is redefined by experimental simulation using a slickwater-alternate-slurry pumping schedule. The modified calculations are proposed to estimate the height of the proppant dune according to the experimental observations. The numerical results are fed into the GRU model for pressure prediction. The errors are analyzed referring to the reference pressure converted from the field measurements. The effects of alternate injection on proppant transport and pressure variation

are evaluated according to the predictions and error analyses.

3.1. Evolution of proppant dune by alternate injection

The proppant dune evolution is recorded and exhibited in Fig. 4. Initially, the slurry is injected into the fracture at a constant rate. The proppant settles down, achieves equilibrium and forms a stratified flow (Fig. 4 a). To control the growth of the proppant dune at the fracture inlet, a flow of pure slickwater is injected to push the proppant moving forward within the fracture, which drags the proppant on the surface and results in a ridge-shape dune (Fig. 4 b). As the slurry and pure slickwater are injected alternately, the ridge can be observed repeatedly (Fig. 4 c and 4 d).

The proppant ridge is a transition state of the proppant dune between the injecting alternation, which is also observed by some previous experiments [33–35]. Previous research focuses on the washout near the inlet, which may lead to fracture closure and conductivity loss. The inducement of the proppant ridge and its effect on proppant transport are neither fully discussed nor linked to the alternate injecting mode. Especially, the proppant dune growing along with the injection schedule (Fig. 4 b to Fig. 4 d) is a key mechanism that is rarely mentioned in previous works. The flowing region (H_1) is compressed into a small channel that increases the velocity of slickwater under a constant pumping rate. The drag force of pure slickwater is enhanced by the increasing velocity [36], which pushes the dune and builds up a higher proppant ridge (Fig. 4 d). Consequently, the fracture connectivity is influenced by the ridge with a height close to the flowing region (H_1). In the field engineering scenario, the frequently-used volume of an injected pure fluid is approximately equal to the wellbore volume aiming to sweep all proppant from the horizontal wellbore into fractures [9]. Such volume of the sweeping fluid may not be sufficient to achieve the equilibrium status of the proppant dune (flat dune) depending on the preceding injected proppant. The ridge-shape dune, therefore, maintains when the following slurry is injected into the fracture, leading to a rapid loss of fracture connectivity and nonnegligible pressure fluctuations. This may be the primary mechanism of how a ridge-shape dune and the slickwater-alternate-slurry pumping schedule affect the proppant injection.

3.2. Modified calculations considering proppant ridge

The height of the flowing region (H_1) above the dune is a key parameter for evaluating the proppant transport status, which may be estimated by the traditional Bi-power model defined as [37].

$$\frac{H_1}{w} = [-0.00023\ln(R_G) + 0.00292]R_f^{1.2-0.00126\lambda^{-0.428}[15.2-\ln(R_G)]} R_P^{[-0.0172\ln(R_G)-0.12]} \tag{1}$$

where H_1 is the height of the flowing region, m; w is the fracture width, which is assigned as $100 \times d_{\max}$ ($d_{\max}$ is the largest diameter of injected proppant) referring to the result of slant core drilling through a stimulated shale reservoir [38], m; R_f, R_p, R_G and λ are calculated by

$$\begin{cases} R_f = \dfrac{\rho_f Q_f}{w\mu} & R_p = \dfrac{\rho_p Q_p}{w\mu} \\ R_G = \dfrac{\rho_f(\rho_p-\rho_f)gd^3}{\mu^2} & \lambda = \dfrac{\mu/\rho_f}{w^{1.5}\sqrt{g}} \end{cases} \tag{2}$$

where ρ_p and ρ_f are densities of proppant and fracturing fluid, respectively, kg/m^3; Q_f and Q_p are the pump rates of fluid and proppant, respectively, m^3/s; μ is the fluid viscosity, Pa·s; d is the averaged diameter of proppant, m.

For an alternate pumping schedule, the accumulated proppant is pushed into deeper fractures when pure fluid is injected. The dune is then rebalanced with a new H_1 given by [39].

$$H_1 = \left(\frac{Q_f\rho_f w^{0.0937}}{2053.4\mu}\right)^{\frac{1}{1.0937}} \tag{3}$$

In our modified calculations, the height of the proppant ridge (H_{ridge}) can be estimated by the flowing region (H_1) and the restarting behaviour of the superficial proppant (Shields number). The expression is proposed as [40].

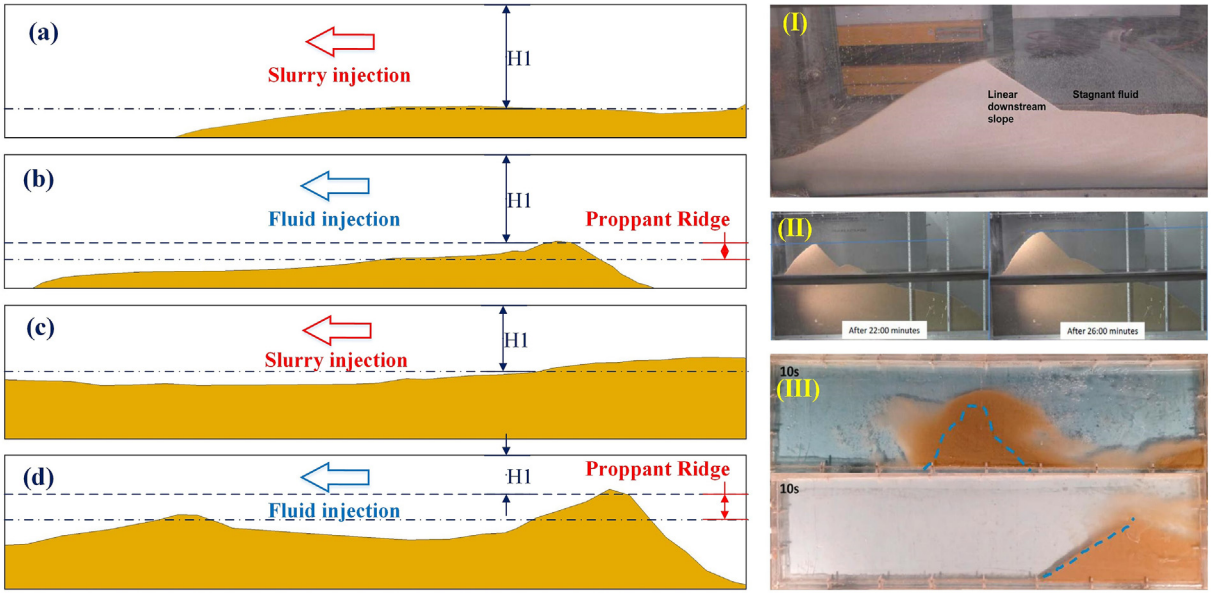

Fig. 4. Schematic of proppant dune evolution under a slickwater-alternate-slurry pumping schedule (left) and previous observations of proppant ridge (right) [33–35].

$$\frac{H_{ridge}}{H_1} = \frac{2S - 0.1}{7S - 0.05} \tag{4}$$

where S is the Shields number and can be calculated by [41].

$$S = \frac{8\mu Q_f}{(\rho_p - \rho_f) g d w^2 H_1} \tag{5}$$

Considering the proppant ridge, the height of the flowing region under the transition status may be proposed as

$$H_1' = H_1 - H_{ridge} \tag{6}$$

In summary, for the traditional Bi-power calculations, Eqs. (1)–(3) are applied to calculate the equilibrium height of the proppant dune (H_1) (Table 2). Our modified calculation, taking into account the height of the proppant bridge, applies Eqs. (1) and (2) and (4)–(6) with the result of H_1' (Table 2). The major difference between the two calculations exists in the process of pure fluid injection, where Eq. (3) is used for the equilibrium state of the proppant dune in the traditional calculations. Correspondingly, Eqs. (4)–(6) are employed for the transition status of the proppant ridge in the modified calculations. The parameters used for calculations include the pump rate and material properties (fluid viscosity, fluid density, proppant diameter and density) that are obtained from field records. Noteworthy, the equations in Table 2 are derived based on the particle settling in the low-viscosity fluid, thus mainly for the application in slickwater. The gel-based fracturing fluid (with high viscosity) suspends the particle and is not suitable for the calculations.

3.3. Pressure prediction for evaluating the proppant transport

The data processing is performed to predict the DPP based on the calculations in Table 2 and the GRU workflow. The proppant transport is evaluated by error analyses (RMSE) of the predictions. The data processing is repeated three times based on the measurements from Platform A to C (Table 1) for averaging the errors. For each iteration, a new GRU model is trained for the prediction. The RMSEs based on testing wells (A_2, B_2 and C_2) are summarized in Table 3. Generally, the mismatches between the GRU predictions and the references are reduced by ~20.2% on average (from 9.60 down to 7.66) as a result of considering the ridge height for the calculations of proppant transport. Moreover, the modified calculations significantly reduce the errors for wells B_2 and C_2.

The DPP predictions and the references (converted from the wellhead pressures) are drawn in Fig. 5. The data before (the period of fracture creation and propagation) and after (the period of fracture closing and fluid permeating after pump-off) proppant injection have been trimmed to mitigate the pressure variation induced by non-proppant-transport factors. The proppant concentrations are presented at the bottom to better interpret the pressure evolution. Overall, the introduction of the ridge height considerably promotes the performance of the GRU workflow. The deviations between predictions and references are significantly improved for all cases at early and late periods of the proppant injection (noted by the dashed circle in Fig. 5).

Table 3
The root mean squared errors (RMSE) based on testing wells.

Well no.	A_2	B_2	C_2	Average
Bi-power calculations	4.25	12.65	11.90	9.60
Modified calculations	3.87	9.48	9.62	7.66

The fracture is initially cracked with an undeveloped volume in the early period and is nearly filled up in the late period. The apparent improvements under those two conditions demonstrate the existence of the proppant ridge (under field conditions) and its significance. In Fig. 5 b and Fig. 5 c, the pressure fluctuates dramatically (showing sawtooth patterns) during the transition period between two alternate injecting phases. In addition, the GRU model based on modified calculations predicts a pressure jump at the late period of proppant injection around 5500 s in the C_2 case, as shown in Fig. 5 c, which may be a precursor to sand screen-out. At the end of this operation, the DPP exceeds 115 MPa and the injected proppant volume has to be halved for safety.

4. Discussions

4.1. Pressure fluctuation by proppant dune evolution

As shown in Fig. 5 a, the pressure fluctuation through the entire injection is relatively small during the operation of well A_2. There may be no substantial change in the flowing region (H_1). The fracture is likely well-developed so that the proppant is transported smoothly within a sufficient volume of flowing channel, comparable to the scenarios shown in Fig. 4 a and Fig. 4 b (the proppant ridge height is relatively small compared with the flowing region). In contrast, different uptrends of pressure variations are observed in Fig. 5 b and Fig. 5 c (based on the field records from wells B_2 and C_2). The proppant concentrations are under 10% compared with that approaching ~20% for well A_2, implying smaller flowing channels within the fractures for wells B_2 and C_2. The proppant ridge may have compressed the flowing region significantly (as illustrated in Fig. 4 c and 4 d) then reduced the fracture connectivity. The pressure, therefore, becomes more sensitive to proppant dune evolution along with the alternate injection and proppant accumulation. The effect of proppant ridge becomes significant on fracturing injection and pressure safety.

In addition, the larger errors remaining in wells B_2 and C_2 may be induced by the continuous fracture propagation during proppant injection. The increasing DPP (Fig. 5 b and 5 c) means the increasing net pressure in fractures, thus boosting the fracture propagation [42]. The fracture variation brings in extra errors in pressure predictions, which results in larger deviations of the curves in Fig. 5 b and Fig. 5 c. The remaining errors in wells B_2 and

Table 2
Integrations of calculations and corresponding inputs/outputs for the GRU workflow.

	Calculations	Inputs of workflow	Outputs of workflow	notes
Bi-power calculations	Eqs. (1)–(3)	H_1 (calculations) + μ, Q, C & d (records)	DPP	Equilibrium state of proppant dune
Modified calculations	Eqs. (1), (2) and (4) (5) & (6)	H_1' (calculations) + μ, Q, C & d (records)		Transition state of proppant ridge

Notes: H_1 – the height of the flowing layer; H_1' – the height of the flowing layer considering proppant ridge; μ – fluid viscosity; Q – pump rate; C – proppant concentration; d – proppant diameter; DPP – the downhole pressure after the perforation.

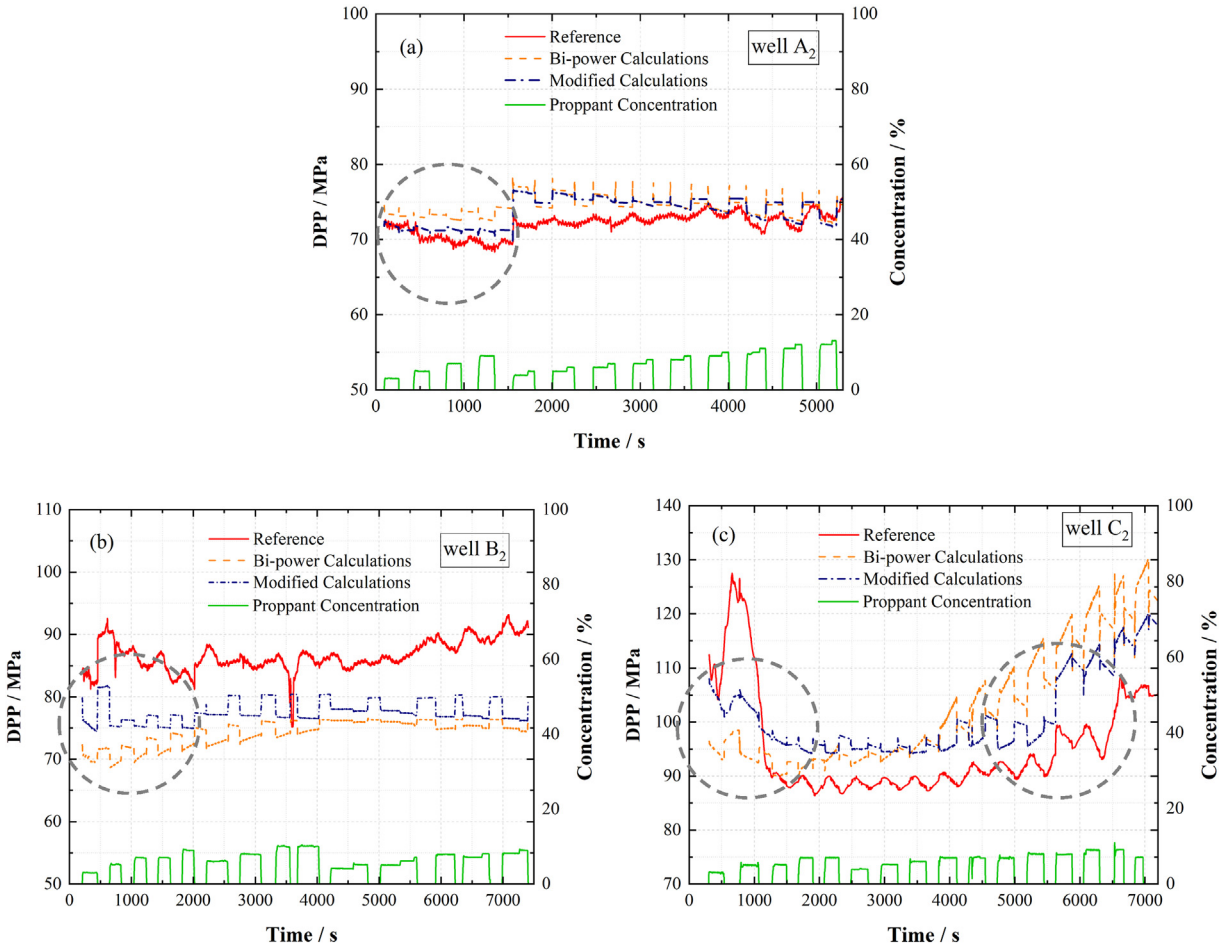

Fig. 5. Prediction and reference (conversion of wellhead measurements) of DDP (downhole pressure after perforation) based on Bi-power and modified (considering the proppant ridge) calculations using data from (a) well A_2, (b) well B_2 and (c) well C_2. The solid red curve is the reference DPP. The solid green curve at the bottom is the proppant concentration that may be useful to analyze the DPP variation. The orange dash curve and the blue dash-dot curve are the GRU predictions based on the Bi-power and modified calculations, respectively. (For interpretation of the references to colour in this figure legend, the reader is referred to the Web version of this article.)

C_2 are beyond the scope of this work since the relative error-improvement is applied for the verification. The precise pressure prediction may require a comprehensive consideration of hydrodynamic, geological and rock-mechanical factors. The discovery of the proppant-ridge-mechanism in this work improves the pressure prediction in the hydrodynamic aspect.

4.2. Sensitivity analysis of proppant ridge height

The parameter sensitivity analysis is conducted using the control variate method. The effects of major hydraulic parameters (pump rate, fluid viscosity, proppant density and diameter) on the proppant ridge height are presented in Fig. 6. The correlation curve for the pump rate shows a positive slope that is much larger than those of the other parameters, indicating a predominant effect of the pump rate on the ridge height. This may also explain the influence of pump rate on sand screen-out, which is peculiarly sensitive under high-rate conditions [19]. An increase in fluid viscosity, representing the value of slickwater and gel, can only slightly promote the growth of the ridge, which is inconsistent with common sense that higher fluid viscosity improves the proppant transport [43]. Smaller diameter and lower density of the proppant may restrain the ridge height. However, the options for proppant types are limited in field applications [4]. It is unlikely to control the ridge height by adjusting proppant and fluid parameters in a real

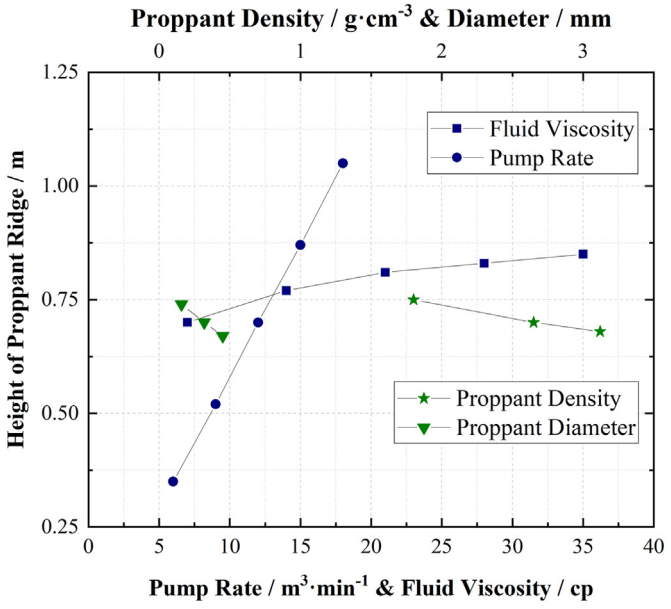

Fig. 6. Effects of injection parameters (pump rate, fluid viscosity, proppant density and diameter) on the height of proppant ridge.

hydraulic fracturing operation. Therefore, a longer pure fluid injection with a lower pump rate may be more efficient for field practices to sweep the proppant deeper into fractures and mitigate the pressure fluctuation induced by the proppant ridge.

4.3. Implications and open questions

The results based on our hybrid approach indicate that the presence of the proppant ridge (induced by the alternate injection) can be critical for proppant transport and corresponding pressure fluctuation. The commonly-used volume of the sweeping fluid (equal to the wellbore volume [9]) is an empirical and rough estimation that considers only the proppant transport in the wellbore. The proportion of the pure slickwater in an alternate pumping schedule should be optimized not only to clean the proppant in the wellbore, but also to control the growth of the proppant ridge in the fracture. This study provides the basis of the proportion optimization for the alternate schedule, such as the pump rate, the growth of the proppant ridge, the flowing region (H_1), etc.

However, the proppant ridge can also be useful to increase the net pressure within fractures, which promotes fracture propagation as long as the operating pressure maintains within a safe level. To better understand the effect of the proppant ridge, more efforts are needed to reveal (1) the effect of various slurry and pure fluid ratios on the accumulating and sweeping process of proppant ridge, which may help to optimize the alternate interval between each phase; (2) the positions along the fracture that intends to generate a ridge; (3) the effect of ridge height and its position on the pressure variations, especially in a highly-filled fracture.

5. Conclusions

A new hybrid approach, involving experiments, calculations and a deep learning workflow (based on the GRU algorithm), is employed to investigate the effect of the slickwater-alternate-slurry pumping schedule on proppant injection. The observation experiment reveals the evolution of the proppant dune, which is then characterized by the modified proppant transport calculations. The calculations connect the experimental mechanism and the GRU workflow by extracting features for training the algorithm. The GRU workflow demonstrates the laboratory discovery and the modified calculations by predicting the denoised pressure (DPP) based on field measurements. This study suggests a promising framework for proppant transport research at field-practical scales, which is more effective for optimizing pumping schedule and enhancing the proppant injection. The main conclusions are generalized as follows:

(1) The ridge-shape proppant dune, a transition status between the alternate injections, is observed through experiments. It is generated by the insufficient volume of the sweeping fluid that fails to achieve the flat equilibrium status of the dune. The proppant ridge erodes the flowing region above the dune, which may obstruct the proppant injection. The modified calculation is proposed to estimate the ridge height. Approximately ~20.2% of the averaged RMSE (GRU predictions) is reduced by considering the ridge height, indicating the significance of the proppant ridge for proppant transport during an alternate injection.

(2) The most remarkable improvements of the GRU predictions are observed in both early and late periods of proppant injection, when fractures are initially cracked with undeveloped volume and nearly filled up, respectively. The flowing region overlying the proppant dune can be significantly compressed or even blocked by the growth of the proppant ridge. Under such conditions, the pressure often fluctuates dramatically and tends to be sensitive to proppant injection, in particular, during the transition period between two alternate injecting phases.

(3) The pump rate, compared with other hydraulic parameters (fluid viscosity, proppant density, and diameter), may dominate the growth of the proppant ridge according to sensitivity analyses of the ridge height. An appropriate reduction in pump rate (for pure slickwater) may be helpful to control the ridge height. Moreover, the alternate interval of the pumping schedule, especially the empirical volume of the sweeping fluid, should be optimized by investigating the evolution of the proppant ridge. Our study highlights the importance of the proppant ridge and defines a promising direction in future studies.

Credit author statement

Lei Hou: Conceptualization, Methodology, Investigation, Writing, Data curation; **Yiyan Cheng**: Data curation; **Xiaoyu Wang**: Methodology, Writing – review & editing; **Jianhua Ren**: Data curation; **Xueyu Geng**: Funding acquisition.

Declaration of competing interest

The authors declare that they have no known competing financial interests or personal relationships that could have appeared to influence the work reported in this paper.

Acknowledgement

This research has received funding from the European Union's Horizon 2020 research and innovation programme under the Marie Sklodowska-Curie grant agreement No. 846775.

Appendix A. Supplementary data

Supplementary data to this article can be found online at https://doi.org/10.1016/j.energy.2021.122987.

References

[1] Nassir M, Settari A, Wan RG. Prediction of stimulated reservoir volume and optimization of fracturing in tight gas and shale with a fully elasto-plastic coupled geomechanical model. SPE J 2014;19(5):771–85.

[2] Hou B, et al. Fracture initiation and propagation in a deep shale gas reservoir subject to an alternating-fluid-injection hydraulic-fracturing treatment. SPE J

2019;24(4). 1,839-1,855.
[3] Mao S, et al. Field-scale numerical investigation of proppant transport among multicluster hydraulic fractures. SPE J 2021;26(1):307–23.
[4] Liang F, et al. A comprehensive review on proppant technologies. Petroleum 2016;2(1):26–39.
[5] Barree R, Conway M. Experimental and numerical modeling of convective proppant transport. In: SPE Annual Technical Conference and exhibition. Society of Petroleum Engineers; 1994.
[6] Tong S, Mohanty KK. Proppant transport study in fractures with intersections. Fuel 2016;181:463–77.
[7] Sahai R, Moghanloo RG. Proppant transport in complex fracture networks–A review. J Petrol Sci Eng 2019;182:106199.
[8] Economides MJ, Nolte KG. Reservoir stimulation, vol. 2. Englewood Cliffs, NJ: Prentice Hall; 1989.
[9] Yew CH, Weng X. Mechanics of hydraulic fracturing. Gulf Professional Publishing; 2014.
[10] Isah A, et al. A comprehensive review of proppant transport in fractured reservoirs: experimental, numerical, and field aspects. J Nat Gas Sci Eng 2021;88.
[11] Hu J, et al. Data-driven early warning model for screenout scenarios in shale gas fracturing operation. Comput Chem Eng 2020:143.
[12] Manchanda R, et al. Integrating reservoir geomechanics with multiple fracture propagation and proppant placement. SPE J 2020;25(2):662–91.
[13] Wei G, et al. A visual experimental study: resin-coated ceramic proppants transport within rough vertical models. J Petrol Sci Eng 2020:191.
[14] Dahi-Taleghani A, Olson JE. Numerical modeling of multistranded-hydraulic-fracture propagation: accounting for the interaction between induced and natural fractures. SPE J 2011;16(3):575–81.
[15] Zhao L, et al. Experimental Study on a new type of self-propping fracturing technology. Energy 2019;183:249–61.
[16] Pahari S, et al. Optimal pumping schedule with high-viscosity gel for uniform distribution of proppant in unconventional reservoirs. Energy 2021:216.
[17] Malhotra S, Lehman ER, Sharma MM. Proppant placement using alternate-slug fracturing. SPE J 2014;19(5):974–85.
[18] Goel N, Shah SN, Grady BP. Correlating viscoelastic measurements of fracturing fluid to particles suspension and solids transport. J Petrol Sci Eng 2002;35(1–2):59–81.
[19] Hou L, et al. Prediction of the continuous probability of sand screen-out based on a deep learning workflow. SPE J 2021. In press.
[20] Hou L, et al. Study of the slippage of particle/supercritical CO2 two-phase flow. J Supercrit Fluids 2017;120:173–80.
[21] Massaras LV, Massaras DV. Real-time advanced warning of screenouts with the inverse slope method. In: SPE formation Damage control International Symposium. LA: Lafayette; 2012.
[22] Nolte KG, Smith MB. Interpretation of fracturing pressures. J Petrol Technol 1981;33(9):1767–75.
[23] Ma L, et al. In-situ synchrotron characterisation of fracture initiation and propagation in shales during indentation. Energy 2021:215.
[24] Cho K, et al. Learning phrase representations using RNN encoder-decoder for statistical machine translation. 2014. arXiv preprint arXiv:1406.1078.
[25] Sagheer A, Kotb M. Time series forecasting of petroleum production using deep LSTM recurrent networks. Neurocomputing 2019;323:203–13.
[26] Fan D, et al. Well production forecasting based on ARIMA-LSTM model considering manual operations. Energy 2021:220.
[27] Gal Y, Ghahramani Z. A theoretically grounded application of dropout in recurrent neural networks. 2015. arXiv preprint arXiv:1512.05287.
[28] Kingma DP, Ba J. Adam: a method for stochastic optimization. 2014. arXiv preprint arXiv:1412.6980.
[29] Zeiler MD. Adadelta: an adaptive learning rate method. 2012. arXiv preprint arXiv:1212.5701.
[30] Hu MY, et al. A cross-validation analysis of neural network out-of-sample performance in exchange rate forecasting. Decis Sci J 1999;30(1):197–216.
[31] Stein RM. Benchmarking default prediction models: Pitfalls and remedies in model validation. New York: Moody's KMV; 2002. p. 20305.
[32] Bergstra J, Bengio Y. Random search for hyper-parameter optimization. J Mach Learn Res 2012;13(2).
[33] Mack M, Sun J, Khadilkar C. Quantifying proppant transport in thin fluids: theory and experiments. In: SPE hydraulic fracturing Technology Conference. Society of Petroleum Engineers; 2014.
[34] Sahai R, Miskimins JL, Olson KE. Laboratory results of proppant transport in complex fracture systems. In: SPE hydraulic fracturing Technology Conference. Society of Petroleum Engineers; 2014.
[35] Chun T, Li Y, Wu K. Comprehensive experimental study of proppant transport in an inclined fracture. J Petrol Sci Eng 2020;184:106523.
[36] Hou L, et al. Incipient motion behavior of the settled particles in supercritical CO2. J Nat Gas Sci Eng 2019;68.
[37] Wang J, et al. Bi-power law correlations for sediment transport in pressure driven channel flows. Int J Multiphas Flow 2003;29(3):475–94.
[38] Elliott SJ, Gale JFW. Analysis and distribution of proppant recovered from fracture faces in the HFTS slant core drilled through a stimulated reservoir. In: Proceedings of the 6th unconventional Resources Technology Conference; 2018.
[39] Patankar NA, et al. Power law correlations for sediment transport in pressure driven channel flows. Int J Multiphas Flow 2002;28(8):1269–92.
[40] Niemann S, Fredsøe J, Jacobsen NG. Sand dunes in steady flow at low Froude numbers: dune height evolution and flow resistance. J Hydraul Eng 2011;137(1):5–14.
[41] Hou L, et al. The key parameters of proppant transport in complex fractures. Chin Sci Bull 2017;62(26):3112–20.
[42] Zhang F, Dontsov E. Modeling hydraulic fracture propagation and proppant transport in a two-layer formation with stress drop. Eng Fract Mech 2018;199:705–20.
[43] Hu YT, Chung H, Maxey JE. What is more important for proppant transport, viscosity or elasticity?. In: SPE hydraulic fracturing Technology Conference. Society of Petroleum Engineers; 2015.